

Reduced storage and balancing needs in a fully
renewable European power system with excess wind
and solar power generation



Dominik Heide, Martin Greiner, Lüder von Bremen
and Clemens Hoffmann

Reduced storage and balancing needs in a fully renewable European power system with excess wind and solar power generation

Dominik Heide^{1,2}, Martin Greiner¹, Lüder von Bremen³
and Clemens Hoffmann⁴

¹Aarhus School of Engineering and Institute of Mathematical Sciences, Aarhus University, Ny Munkegade 118, 8000 Aarhus C, Denmark

²Frankfurt Institute for Advanced Studies (FIAS) and Frankfurt International Graduate School for Science, Johann Wolfgang Goethe Universität, Ruth-Moufang-Straße 1, 60438 Frankfurt am Main, Germany

³ForWind – Center for Wind Energy Research, University of Oldenburg, Marie-Curie-Str. 1, 26129 Oldenburg, Germany

⁴Corporate Research and Technology, Siemens AG, 81730 München, Germany

Abstract

The storage and balancing needs of a simplified European power system, which is based on wind and solar power generation only, are derived from an extensive weather-driven modeling of hourly power mismatches between generation and load. The storage energy capacity, the annual balancing energy and the balancing power are found to depend significantly on the mixing ratio between wind and solar power generation. They decrease strongly with the overall excess generation. At 50% excess generation the required long-term storage energy capacity and annual balancing energy amount to 1% of the annual consumption. The required balancing power turns out to be 25% of the average hourly load. These numbers are in agreement with current hydro storage lakes in Scandinavia and the Alps, as well as with potential hydrogen storage in mostly North-German salt caverns.

Keywords: energy system design, wind power generation, solar power generation, large-scale integration, storage

Corresponding author: Martin Greiner, greiner@imf.au.dk

1 Introduction

A fully renewable European power system will be based on various forms of renewable power generation, with a dominant contribution from wind and solar power. These two weather-driven energy sources come with strong temporal fluctuations. In order to absorb these fluctuations, enormous amounts of storage and balancing are required. For a simplified European scenario based on 100 % wind and solar power generation the required storage energy capacity has been estimated [1]. Depending on the round-trip storage technology, it amounts to 12 %–15 % of the annual European consumption. Given the consumption rate of 2007, this corresponds to 400 TWh–480 TWh. This number is already an optimal minimum, where 60 % wind and 40 % solar power generation are mixed, so that their opposite strong seasonal dependences almost cancel each other and follow the weaker seasonal behavior of the load. For a 100 % wind-only as well as a 100 % solar-only scenario the required storage energy capacity has been estimated to be twice as much.

A storage energy capacity of several hundred TWh represents an incredibly large number. For pumped hydro and compressed air storage in Europe this is fully out of reach [2, 3]. A hypothetical hydrogen storage in mostly North German salt caverns has a potential of a few tens of TWh [4], but even this would still be more than one order of magnitude below the estimate. At present no other large-scale round-trip storage technologies are in sight. – Hydro storage lakes represent a different form of storage. Like gas plants, they do not store excess electricity, but are able to balance electricity deficits. Norway, Sweden, Austria and Switzerland have most of the storage lakes in Europe, with an annual balancing energy of about 150 TWh [5]. Also this is by far not sufficient to match the required amount, which has not been calculated in Ref. [1], but which will be larger than the required energy capacity of 400 TWh–480 TWh for roundtrip storage.

A solution has to be found how to reduce the enormous amount of storage needs for a fully renewable European power system. A straightforward part of this solution is to allow, on average, excess wind and solar power generation. Negative, hourly power mismatches in the fluctuating balancing between the combined wind and solar power generation and load will occur less frequently, thus lowering the need for storage. By using the same modeling approach as in Ref. [1], this paper provides quantitative estimates on how the storage and balancing capacities decrease as a function of excess power generation. In addition to energy capacity for roundtrip storage, it also considers the annual balancing energy required for hydro storage lakes or gas power plants, as well as the balancing power, which is another important storage characteristics.

Besides the dependence on excess generation, it is also interesting to look at the dependence on the mixing ratio between wind and solar power generation. The minimization of storage energy capacity, balancing energy and balancing power can be seen as three different optimization objectives. Those may result in different optimal mixes between wind and solar power generation. This paper is also addressing this issue. It provides an explanation for the differing outcomes and, with a simple time-scale analysis, clarifies under which conditions these optimal mixes may become identical.

The structure of the paper is as follows: Section 2 focuses on the required energy capacity for roundtrip storage. Estimates on the required annual balancing energy are given in Section 3. The balancing power, or discharge power, is discussed in Section 4. Section 5 introduces a separation of time scales, which allows to distinguish between long- and short-term storage needs. The conclusion and an outlook is presented in Section 6.

2 Storage energy capacity as a function of excess generation

The modeling approach of Ref. [1] provides tempo-spatial pattern sequences of wind power generation, solar power generation and load over all of Europe, with a $47 \text{ km} \times 48 \text{ km}$ spatial resolution and 1 h temporal resolution over the 8-year-period 2000–2007. Complete spatial aggregation produces time series of the total European wind power generation $W(t)$, solar power generation $S(t)$ and load $L(t)$. An arbitrary one-year and one-month period is illustrated in Figure 1. For convenience, throughout this paper, all time series have been normalized to their average value, so that $\langle W \rangle = \langle S \rangle = \langle L \rangle = 1$.

The hourly power mismatch,

$$\Delta(t) = \gamma [aW(t) + (1 - a)S(t)] - L(t), \quad (2.1)$$

is key to determine the required storage needs. For $\gamma > 1$, $(\gamma - 1) \geq 0$ represents the average excess generation. a and $(1 - a)$ are equal to the share of average wind- and solar-power generation, respectively. Figure 2 (top) visualizes the hourly power mismatch for a specific combination of a and γ .

Whenever the mismatch is positive, the excess generation can be stored with efficiency η_{in} . In case of a negative mismatch, the generation deficit can be taken out of the storage with efficiency η_{out} . This defines a simple storage model:

$$H(t) = H(t - 1) + \begin{cases} \eta_{\text{in}}\Delta(t) & \text{if } \Delta(t) \geq 0, \\ \eta_{\text{out}}^{-1}\Delta(t) & \text{if } \Delta(t) < 0. \end{cases} \quad (2.2)$$

The time series $H(t)$ describes the filling level of a non-constrained storage. It works fine for parameter settings γ , η_{in} , η_{out} , where the average power generation minus storage losses exactly matches the average load. For such settings, a simple model for the minimum sufficient storage energy capacity can be expressed as [1]: $E_{\text{H}} = \max_t H(t) - \min_t H(t)$.

However, for parameter settings, where on average power generation minus storage losses is larger than load, the fluctuating storage level (2.2) will drift in time; see Fig. 2 (middle). In such cases, the simple subtraction of the overall minimum from the overall maximum of the storage-level time series does not make sense. The new definition:

$$E_{\text{H}} = \max_t (H(t) - \min_{t' \geq t} H(t')) . \quad (2.3)$$

takes care of the positive drift. At time t the non-constrained storage level is $H(t)$. For all larger times $t' \geq t$ the non-constrained storage level does not drop below

$\min_{t' \geq t} H(t')$. Their difference represents the required stored energy at time t . Its maximum over all times yields the required overall storage energy capacity E_H .

With the definition (2.3), the non-constrained time series (2.2) can be transformed into a constrained storage-level time series:

$$H_c(t) = \begin{cases} E_H & \text{if } E_H - H_c(t-1) < \eta_{\text{in}}\Delta(t) , \\ H_c(t-1) + \eta_{\text{in}}\Delta(t) & \text{if } E_H - H_c(t-1) > \eta_{\text{in}}\Delta(t) > 0 , \\ H_c(t-1) + \eta_{\text{out}}^{-1}\Delta(t) & \text{if } \Delta(t) \leq 0 . \end{cases} \quad (2.4)$$

By construction, the constrained storage level never exceeds the energy storage capacity (2.3) and, for a sufficiently large initial value $0 < H_c(0) \leq E_H$, never drops below zero. An example of a constrained storage level time series is shown in Fig. 2 (bottom). Whenever the constrained storage is full, it discards excess power. This is the main difference to the unconstrained storage.

Via (2.1) and (2.2), the storage energy capacity (2.3) depends on the excess generation γ and the relative share a of wind power generation. This dependence is illustrated in Fig. 3a. The storage efficiencies have been set to $\eta_{\text{in}} = \eta_{\text{out}} = 1$. The contour plot reveals a strong dependence on a and γ . At $\gamma = 1$ the minimum storage energy capacity is at $a \approx 0.6$. This reproduces the optimal mix between wind and solar power generation found in Ref. [1]. As can be seen from the dashed line, the optimal mix depends on γ . For $1.1 \leq \gamma \leq 1.4$ it is around $a \approx 0.75$ and for $1.6 \leq \gamma \leq 1.9$ it is around $a \approx 0.45$. Fig. 3b shows several one-dimensional cuts through the two-dimensional landscape of Fig. 3a. The cuts along the optimal mix and along $a = 0.6$ are almost identical. For these two cases the storage energy capacity decreases much faster with increasing γ than along the wind-only $a = 1$ and solar-only $a = 0$. At $\gamma = 1.05$ the storage energy capacity $E_H(\gamma = 1.05, a = 0.6)$ is half of $E_H(\gamma = 1, a = 0.6)$, at $\gamma = 1.15$ it is a quarter, and at $\gamma = 1.35$ it is a tenth; see also Tab. 1.

Fig. 4 is similar to Fig. 3, except that the storage efficiencies have been set to $\eta_{\text{in}} = \eta_{\text{out}} = 0.6$, yielding a roundtrip efficiency of 0.36 valid for hydrogen storage [4]. Due to the conversion losses, some extra generation is needed to make up for the losses. The left border in Fig. 4a represents the extra generation in order to fully match the average load. For $a = 1.0, 0.7$ and 0.0 this extra generation amounts to $\gamma = 1.23, 1.20$ and 1.87 , respectively. Again, the storage energy capacity reveals a strong dependence on a and γ . The optimal mix between wind and solar power generation is at $a \approx 0.7$. Compared to $E_H(\gamma = 1.20, a = 0.7)$, the storage energy capacity $E_H(\gamma, a = 0.7)$ reduces to a half at $\gamma = 1.23$, to a quarter at 1.30 , and to a tenth at 1.57 ; see Fig. 4b and Tab. 1. The wind-only storage energy capacity $E_H(\gamma, a = 1.0)$ is found to be significantly larger than for the optimal-mix storage energy capacity $E_H(\gamma, a = 0.7)$. The solar-only storage energy capacity $E_H(\gamma, a = 0.0)$ is beyond reach.

The storage energy capacity in Figs. 3 and 4 is measured in annual consumption. The average annual consumption for all of Europe has been 3240 TWh in 2007. In case of ideal storage efficiencies, the value $E_H(\gamma = 1.00, a = 0.6) = 0.10$ then corresponds to 330 TWh of stored energy. With 35 % excess generation this value is reduced to a tenth, i.e. $E_H(\gamma = 1.35, a = 0.6) = 33$ TWh. Because of the conversion losses, hydrogen storage requires 20 % excess generation per se. Its storage energy

capacity $E_H(\gamma = 1.20, a = 0.7) = 0.12$ corresponds to 400 TWh. A 57% excess generation is needed to reduce this value down to $E_H(\gamma = 1.57, a = 0.7) = 40$ TWh.

3 Balancing energy as a function of excess generation

Balancing generators are different to roundtrip storage. Examples are storage lakes and gas turbines. They do not make use of the positive power mismatch and are only used to balance the negative mismatch.

The negative mismatch defines the hourly balancing power:

$$B(t) = \begin{cases} -\Delta(t) & \text{if } \Delta(t) < 0, \\ 0 & \text{otherwise.} \end{cases} \quad (3.1)$$

When multiplied with the number of hours $T = 8760$ contained in a year, its average leads to a measure:

$$E_B = \langle B \rangle T, \quad (3.2)$$

which we denote as the annual balancing energy.

Fig. 5 illustrates E_B as a function of the excess generation γ and the relative share a of wind-power generation. The contour plot reveals that E_B has a minimum at $a \approx 0.8$ for all γ . Compared to its E_H counterpart at $a \approx 0.6$, this optimal mix is shifted towards a larger fraction of wind power generation.

In order to understand this, we introduce the daily average profile for wind and solar power generation and load, which we denote $w(t)$, $s(t)$ and $l(t)$ respectively. These are calculated as the average power generation or load at a particular hour during the day ($0 < t \leq 24$) for the entire 8-year-period. The profiles are illustrated in Fig. 6a together with selected combinations of the form $aw(t) + (1 - a)s(t)$. As expected, solar power generation peaks during midday with no generation at night time, wind power generation is slightly higher during night time and the load is higher during day time; see also the respective time series of Fig. 1b, where these effects are also observed. The difference

$$E_{\text{profile}} = \frac{1}{2 \cdot 24} \sum_{t=1}^{24} |l(t) - [aw(t) + (1 - a)s(t)]| \quad (3.3)$$

of the profiles represents a measure for the balancing needs at $\gamma = 1$. Fig. 6b shows E_{profile} as a function of the wind power fraction a and reveals a minimum at $a = 0.92$. Revisiting Fig. 6a, we see that the profile with $a = 0.9$ represents a close match to the load profile.

Also shown in Fig. 6b is a comparison between $E_{\text{profile}}(a)$ and the balancing energy $E_B(a, \gamma = 1)$. Up to $a \approx 0.6$ both quantities are almost identical, but beyond that they differ. At $a = 0$ the solar-only profile exceeds the load profile during day times and is zero during night times. In other words, no balancing is needed for half of the day and full balancing is needed for the other half of the day. This explains $E_{\text{profile}}(a = 0) \approx E_B(a = 0, \gamma = 1) \approx 0.5$. The small difference between the two quantities is due to fluctuations of the solar power generation, which are

present on hourly, daily and seasonal time scales. In the other limit, $a = 1$, only fluctuations due to wind power generation are present. These have a big impact on the balancing energy. $E_B(a = 1, \gamma = 1) = 0.19$ is about three times as large as $E_{\text{profile}}(a = 1) = 0.06$. The large difference can be explained by the strong seasonal behavior of the wind resource. Furthermore, the minimum of $E_{\text{profile}}(a)$ at $a = 0.92$ is shifted to $a = 0.81$ for $E_B(a, \gamma = 1)$.

Figure 5b shows the dependence of the annual balancing energy on γ for various fixed a . $a = 1$ and $a = 0.6$ lead to an almost identical behavior. With only solar power generation ($a = 0$) the required balancing energy becomes much higher - close to 50 % of the annual consumption. This is much larger than for $0.6 \leq a \leq 1.0$. For $a = 0.8$ the balancing energy decreases from 15 % of the annual consumption at $\gamma = 1$ to 10 % at $\gamma = 1.18$ and 5 % at $\gamma = 1.49$. Considering again the annual European consumption of 3240 TWh for the year 2007, 15 %, 10 % and 5 % translate into required annual balancing energies of 480 TWh, 320 TWh and 160 TWh, respectively. A balancing energy of 100 TWh requires an excess generation $\gamma = 1.72$ at $a = 0.8$.

4 Balancing power as a function of excess generation

The estimates in Sections 2 and 3 have addressed the required amount of storage energy capacity and annual balancing energy. An equally important characteristic of a future power system based solely on wind and solar power generation is balancing power, which can also be seen as discharge power. The driving questions are: how large can the hourly power mismatches become, and how often do they occur? In more general terms, what is the statistics of the balancing power $B(t)$ (see Eq. (3.1)), and how does it depend on a and γ ?

Figure 7 illustrates the probability distributions $p(B)$ of the hourly balancing power $B(t)$ for selected combinations of a and γ , sampled over the entire eight years of available data. All distributions have a pronounced peak at $B = 0$. For $\gamma = 1$ the peaks have a probability mass 0.47, 0.49, 0.46, 0.39 at $a = 1, 0.8, 0.6, 0$, indicating that balancing is needed for a little more than 50 % of the time. For $\gamma = 1.5$ we find 0.73, 0.79 and 0.70 for $a = 1, 0.8$ and 0.6 , indicating that balancing is needed for about 25 % of the time. In case of the solar-only $a = 0$, the distributions are almost independent of γ . During day hours the solar power generation exceeds the load, which again explains the peak at $B = 0$ with probability mass ≈ 0.4 . During night hours no sun is shining, with the consequence that independent of the value for γ full balancing is required. The maximum balancing results to be $\max_t B(t) = 1.4$ times the average hourly load. The maximum balancing for the wind-only $a = 1$ is smaller. It turns out to be $\max_t B(t) = 1.12$ for $\gamma = 1$ and decreases a little to 1.01 for $\gamma = 1.5$. The probability distributions for $a = 1$ are very similar to those with $a = 0.6$. For values between $a = 1$ and 0.6 , the tail of the distribution is slightly shifted to smaller values.

The average of these distributions has already been shown in Fig. 5. Figure 8a illustrates the 99 % ($q = 0.99$) quantile Q_B as a function of a and γ . It is defined as $\int_0^{Q_B} p(B)dB = q$. For every γ its minimum lies at $a = 0.88$. Along this minimum

line, the 99 % quantile $Q_B(a = 0.88, \gamma)$ decreases linearly with γ , from 70 % of the average hourly load at $\gamma = 1$ down to 35 % at $\gamma = 2$. These rather large values guarantee that 99 % of the time, the hourly balancing power remains below these quantiles. In other words, in 1 % of the time, or 1.7 hours per week, the hourly balancing power will be larger than 70 % ($\gamma = 1$) or 35 % ($\gamma = 2$) of the average hourly load. Fig. 8b depicts other quantiles for $\gamma = 1.5$. The quantile with $q = 0.999$ means that only nine hours within one year result in a larger balancing power. The optimal a , which minimizes the quantile, increases with q . For $q = 0.9, 0.99$ and 0.999 , it turns out to be $a = 0.85, 0.88$ and 0.90 , respectively.

Table 1 summarizes the hourly 90 %, 99 %, 99.9 % balancing quantiles for all combinations of $a = 0.6, 0.7, 0.8$ and 0.9 and $\gamma = 1, 1.25$ and 1.5 in units of the average hourly load. Given again the annual European consumption of 3240 TWh in the year 2007, the average hourly load amounts to 370 GW. For the 99 % quantiles with $a = 0.6$ and $\gamma = 1$ or 1.5 , this translates to 300 GW or 240 GW, respectively.

5 From hourly to daily power mismatches

When looking at Figures 3a, 4a, 5a and 8a, we observe that storage energy capacity, annual balancing energy and balancing quantile come with differing optimal combinations between wind and solar power generation; consult also Tab. 1. The minimum of E_H is at $a \approx 0.5$ to 0.7 , the minimum of E_B at $a \approx 0.8$, and the minimum of the 99 % quantile Q_B at $a \approx 0.9$. This can be seen as the result of three different optimization objectives.

The explanation for these differences is revealed by Figure 9. It depicts the temporal fluctuation pattern of balancing power over all hours and days of one full year for various combinations of a and γ . These patterns result from combinations of patterns for wind power generation, solar power generation and load. The latter three are illustrated in Figure 10. Since they are very different from each other, different combinations of the form (2.1) lead to different fluctuation patterns for the balancing power (3.1). As can be seen in the first row of Figure 9, the limit $a \approx 1$ is dominated by the wind pattern of Figure 10a. The limit $a \approx 0$ is shown in the last row of Figure 9 and is dominated by the solar pattern of Figure 10b. The fluctuation patterns in the intermediate regime $a \approx 0.6$ – 0.8 are inbetween the two extremes. The second and third rows of Figure 9 reveal that almost no balancing is needed during daylight times. Only during night hours a reduced balancing is needed.

The fluctuation patterns of Figure 9 reveal a regular intra-day power-mismatch behavior for $0 \leq a \leq 0.9$. Excess power is generated during daytime and negative power mismatches occur during nighttime. This regular intra-day behavior has a big impact on the objective to minimize balancing energy and power. If we were to average over this intra-day behavior and switch from hourly to daily mismatches, then the respective optimal mixes will change.

In the following, the hourly time resolution of the wind power generation $W(t)$, the solar power generation $S(t)$, the load $L(t)$, the power mismatch $\Delta(t)$ and the balancing power $B(t)$ will be changed to one day. The daily wind power generation

then is:

$$\overline{W}(\tau) = \frac{1}{24} \sum_{t=24(\tau-1)+1}^{24\tau} W(t) ; \quad (5.1)$$

it is divided by 24 in order to normalize its average to one. The time τ proceeds in steps of one day. The daily solar power generation $\overline{S}(\tau)$ and the daily load $\overline{L}(\tau)$ are obtained in complete analogy. The daily mismatch too can be calculated directly from the hourly mismatch by substituting $W(t)$ for $\Delta(t)$ in (5.1) or it can be calculated from the daily averages as:

$$\overline{\Delta}(\tau) = \gamma [a\overline{W}(\tau) + (1-a)\overline{S}(\tau)] - \overline{L}(\tau) . \quad (5.2)$$

However, the daily balancing power must be calculated from the daily mismatch:

$$\overline{B}(\tau) = \begin{cases} -\overline{\Delta}(\tau) & \text{if } \overline{\Delta}(\tau) < 0 \\ 0 & \text{otherwise,} \end{cases} \quad (5.3)$$

which is not identical to the daily average of the hourly balancing power. Actually $\overline{B}(\tau)$ is smaller than $(1/24) \sum_{t=24(\tau-1)+1}^{24\tau} B(t)$, because the latter does not take into account the compensating positive mismatches occurring over the day.

Based on the daily mismatch $\overline{\Delta}(\tau)$ and the daily balancing power $\overline{B}(\tau)$, the storage energy capacity, the annual balancing energy and the balancing quantiles are determined completely analogous to Sections 2–4. The results are shown in Figure 11 as a function of γ and a .

Figure 11a and Figure 3a are indistinguishable, which means that the ideal ($\eta_{\text{in}} = \eta_{\text{out}} = 1$) storage energy capacities based on hourly and daily mismatches are identical; compare also the third columns of Tables 1 and 2. As can be seen from the storage level time series of Figures 2b+c, the storage energy capacity is only determined by fluctuations on the synoptic and seasonal time scales, which are larger than one day. The optimal mix associated with minimum storage energy capacity is not affected by the change from hourly to daily mismatches.

For hydrogen storage with reduced efficiencies $\eta_{\text{in}} = \eta_{\text{out}} = 0.6$ the storage energy capacities based on daily and hourly mismatches are not identical; compare Figure 11b and Figure 4a. They are similar for $0.85 \leq a \leq 1$, but differ for $0 \leq a \leq 0.85$. This difference is specified in the fourth columns of Tables 1 and 2. The optimal mix between wind and solar power generation is slightly moved from $a \approx 0.7$ to $a \approx 0.6$ when switching from hourly to daily mismatches.

Figures 11c+d illustrate the annual balancing energy and the 99% balancing quantile based on the daily mismatches. They are completely different from their counterparts based on the hourly mismatches; consult again Figures 5a and 8a. Independent of γ the new minima are found at $a \approx 0.5$.

These results demonstrate nicely that the choice of time resolution has an impact on the optimal mixes; see also Ref. [6], where the optimal mix has been defined in terms of the mismatch variability. Based on the hourly mismatches, the optimal mixes $a \approx 0.6$, 0.8 and 0.9 for storage energy capacity, annual balancing energy and balancing power turn out to be different. Once the pronounced daily profile of the hourly mismatches is filtered out by going over to daily mismatches, the optimal mixes become almost identical around $a \approx 0.5$ – 0.6 .

Based on the daily mismatches, Table 2 lists the obtained values for the storage energy capacity E_H , the annual balancing energy E_B and the balancing quantiles Q_B for various combinations of γ and a . Compared to the hourly mismatches, the daily-based storage energy capacity with ideal efficiencies $\eta_{in} = \eta_{out} = 1$ is not reduced, and with lower efficiencies $\eta_{in} = \eta_{out} = 0.6$ it is slightly reduced. On the other hand, the annual balancing energy and the quantiles of balancing power are greatly reduced. The E_B values 0.094, 0.028 and 0.009 for $a = 0.6$ and $\gamma = 1, 1.25$ and 1.5 are significantly smaller than the respective 0.153, 0.084 and 0.049 for the hourly-based E_B at its minimizing $a = 0.8$. A similar finding is obtained for the balancing quantiles, where for example the 0.526 and 0.716 of the hourly-based 99% and 99.9% quantiles Q_B at $\gamma = 1.5, a = 0.9$ are reduced by a factor of two down to 0.246 and 0.364 for the respective daily-based quantiles at $a = 0.6$.

Figure 12 summarizes the results obtained in Figure 11 and Table 2 in a different way. For fixed $a = 0.6$ it compares the γ dependence of the smaller daily-based with the larger hourly-based storage energy capacities, annual balancing energies and balancing quantiles. With this comparison we are tempted to distinguish between a long-term and a short-term storage.

The long-term storage takes care of the daily mismatch. Its storage energy capacity, or annual balancing energy, and power quantiles correspond to those based on the daily mismatches. With another look into Table 2 at for example $\gamma = 1.5$ and $a = 0.6$ the required numbers are $E_H(\eta = 1) = 0.004$ and $Q_B(q = 0.99) = 0.246$ for ideal round-trip storage, which, given the annual European consumption of 2007, translate into $E_H(\eta = 1) = 15$ TWh and $Q_B(q = 0.99) = 90$ GW. For hydrogen storage the respective numbers are $E_H(\eta = 0.6) = 0.010 = 35$ TWh and $Q_B(q = 0.99) = 0.246 = 90$ GW. Note, that the quantile $Q_B(q = 0.99)$ can be seen as the discharge power. For balancing generators, like hydro storage reservoirs or gas power plants, the respective numbers are $E_B = 0.009 = 30$ TWh and $Q_B(q = 0.99) = 0.246 = 90$ GW.

The short-term storage takes care of the hourly power mismatch around the daily mismatch. The difference between the quantile based on the hourly mismatch and the quantile based on the daily mismatch represents a lower bound for the required balancing power. Again for $\gamma = 1.5$ and $a = 0.6$, this results in $Q_B^{\text{hourly}}(q = 0.99) - Q_B^{\text{daily}}(q = 0.99) = 0.40 = 140$ GW. A rough number for the required energy capacity for a short-term roundtrip storage would then be $E_H^{\text{short-term}} \approx 140 \text{ GW} \times 12 \text{ h} = 1.68 \text{ TWh} \approx 2 \text{ TWh}$. Candidates for such a short-term storage would be pumped hydro, electric cars and other batteries, compressed air, and any combination thereof.

6 Conclusion and outlook

Based on extensive weather-driven modeling of hourly mismatches between wind plus solar power generation and load, we have given estimates on the storage needs for a fully renewable European power system. Depending on the objectives to minimize storage energy capacity, annual balancing energy or balancing power, different optimal mixes between wind and solar power generation have been found. In case of storage energy capacity, the optimal mix is 60% wind and 40% solar power generation for ideal roundtrip storage, and 70% wind and 30% solar power generation for

hydrogen storage. In case of annual balancing energy, the optimal mix is 80 % wind and 20 % solar power generation. In case of balancing power, the optimal mix is 90 % wind and 10 % solar power generation. These optimal mixes turn out to be more or less independent from the amount of excess power generation. The difference of the three optimal mixes is mainly caused by the intra-day mismatch dynamics. Once the intra-day time scales are neglected by considering daily instead of hourly power mismatches, the optimal mixes for storage energy capacity, annual balancing energy and balancing power collapse onto each other and become identical with 60 % wind and 40 % solar power generation.

With no excess wind plus solar power generation, the required storage and balancing needs based on the hourly power mismatches turn out to be very large. However, they decrease very fast with the introduction of excess power generation. Given the annual European consumption of 3240 TWh for 2007 and given the objective to minimize the storage energy capacity, the required needs for roundtrip storage with ideal efficiencies $\eta_{\text{in}} = \eta_{\text{out}} = 1$ amount to $E_{\text{H}} = 320$ TWh energy capacity and $Q_{\text{B}}(q = 0.99) = 300$ GW discharge power for $\gamma = 1$ and $a = 0.6$. For excess generation with $\gamma = 1.5$ and $a = 0.6$ these numbers reduce to $E_{\text{H}} = 16$ TWh and $Q_{\text{B}}(q = 0.99) = 240$ GW. However, from $\gamma = 1$ to 1.5 the installed wind and solar-photovoltaic power capacities across Europe would each increase from 750 GW to 1100 GW.

For comparison, hydrogen storage with non-ideal efficiencies $\eta_{\text{in}} = \eta_{\text{out}} = 0.6$ would require 50 TWh and 220 GW for energy capacity and discharge power, respectively. This scenario is for $\gamma = 1.5$ and $a = 0.7$ with installed 1300 GW wind and 830 GW solar power capacities. If we were to choose the other objective to minimize the discharge power, then the optimal $a = 0.9$ at $\gamma = 1.5$ leads to a required storage energy capacity of 120 TWh and a discharge power of 195 GW, with installed 1650 GW wind and 275 GW solar power capacities.

For balancing generators, like storage lakes and gas power plants, the two objectives to minimize either the balancing energy or the balancing power lead to quite similar results. The optimal share of generated wind power amounts to $a \approx 0.8$ -0.9. At zero excess generation $\gamma = 1$ the required European annual balancing energy and balancing power result to be 510 TWh and 265 GW, respectively. These numbers are reduced down to 160 TWh and 200 GW once the excess generation is increased to $\gamma = 1.5$.

The presented results demonstrate that excess wind and solar power generation can be used to significantly reduce the required storage needs for a fully renewable European power system. However, with a 50 % excess power generation the resulting storage energy capacity, annual balancing energy and balancing power are still very large. What are the possibilities in Europe, now and in the future? The storage lakes in Norway, Sweden, Austria and Switzerland currently have an annual balancing energy of about 150 TWh with a balancing power of about 55 GW [5]. Hypothetical large-scale hydrogen storage would take place in salt caverns, which nowadays are widely used for gas storage. A typical large cavern field has a volume of $8 \times 10^6 \text{ m}^3$ [3, 4], which, given the volumetric energy storage density of 170 kWh/m³ for hydrogen, would provide a storage energy capacity of 1.3 TWh with a discharge power of about 2.6 GW. Mainly North Germany, but also Denmark, the Netherlands and Great

Britain certainly have the potential for some more of these salt cavern fields. Twenty of them would provide a storage energy capacity of 25 TWh with a discharge power of 50 GW.

These numbers for the current hydro storage lakes and the hypothetical hydrogen storage are not so far away from the previous estimates based on 50% excess generation. The latter converge even further once both technologies are thought of as long-term storage only. For one-way storage reservoirs and $\gamma = 1.5$ the required annual balancing energy and power based on daily, instead of hourly power mismatches turn out to be 30 TWh and 90 GW, respectively. The same numbers are estimated for the energy capacity and discharge power of long-term hydrogen storage. Given these results, it appears that a combination of hydro storage lakes and hydrogen storage will be able to contribute solving Europe's search for a long-term storage.

Of course, hydro storage lakes and hydrogen storage alone will not be able to deliver an implementable solution for a fully renewable European power system. Additional technology is required. So far, we have treated Europe as one big copper-plate. Power transmission across Europe is needed to balance local negative power mismatches with positive mismatches in other regions and to allow for flows into and out of the long-term storage locations. Another important topic focuses around the question, what to do with the excess wind and solar power generation. A quite natural route will be to strongly couple the future electricity sector to the heating (and cooling) as well as the transportation sector. Last but not least, the development of a renewable energy picture for a future Europe needs to be evaluated from a macro-economical perspective [7].

Acknowledgements

We thank Markus Speckmann, Stefan Bofinger, Kaspar Knorr, Bernhard Lange and Kurt Rohrig for several discussions during the early phase, and Jan Scholz, Mirko Schäfer, Morten Rasmussen, Gorm Andresen and Fritz Crotogino for several discussions during the late phase of our research leading to this Paper.

References

- [1] D. Heide, L. von Bremen, M. Greiner, C. Hoffmann, M. Speckmann, S. Bofinger, *Renewable Energy* 35 (2010) 2483–2489.
- [2] EURPROG 2005, Network of Experts, Statistics and prospects for the European electricity sector (1980–1990, 2000–2020), Union of the Electricity Industry (Eurelectric) (2005).
- [3] London Research International, Survey of energy storage options in Europe. Report, March 2010.
- [4] S. Donadei, F. Crotogino, Energy storage in salt caverns – today and tomorrow. 9th World Salt Symposium, Beijing, China, 04–09 September 2009.

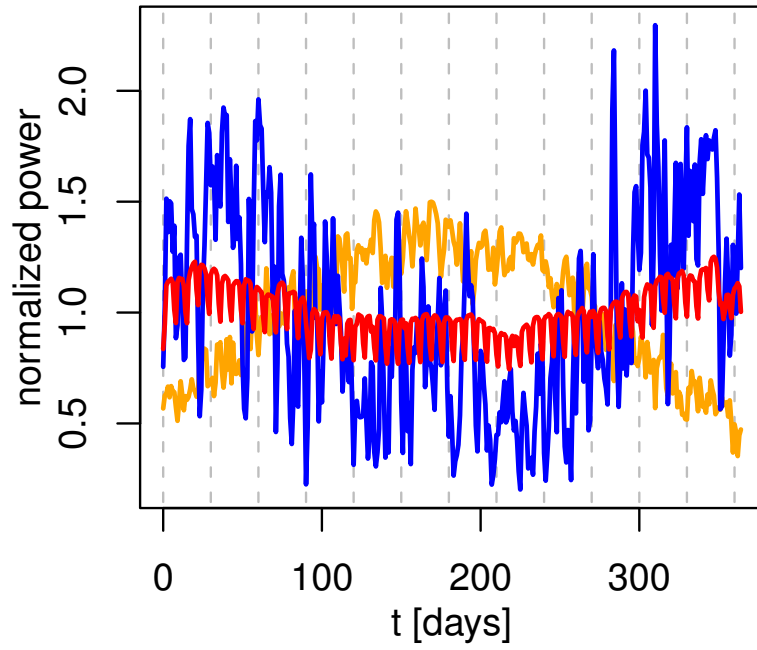
- [5] K. Wiedemann, Einmal Fjord und zurück. *Neue Energie*, 07/2010, pp. 24–31.
- [6] L. von Bremen, Large-scale variability of weather-dependent renewable energy sources. NATO science for peace and security series -C: environmental security. Ed. by A. Troccoli, *Management of weather and climate risk in the energy industry*. Springer, ISBN 978-90-481-3690-2 (2010).
- [7] T. Aboumahboub, K. Schaber, P. Tzscheutschler, T. Hamacher, Optimal configuration of a renewable-based electricity supply sector, *WSEAS Transactions on Power Systems* 2 (2010) 120–129.

Table 1: Storage energy capacity E_H , annual balancing energy E_B , and hourly 90%, 99% and 99.9% balancing quantiles Q_B for all combinations of $a = 0.6, 0.7, 0.8, 0.9$ and $\gamma = 1, 1.25, 1.5$. The storage energy capacity and annual balancing energy are normalized to the average annual consumption. The balancing quantiles are normalized to the average hourly load.

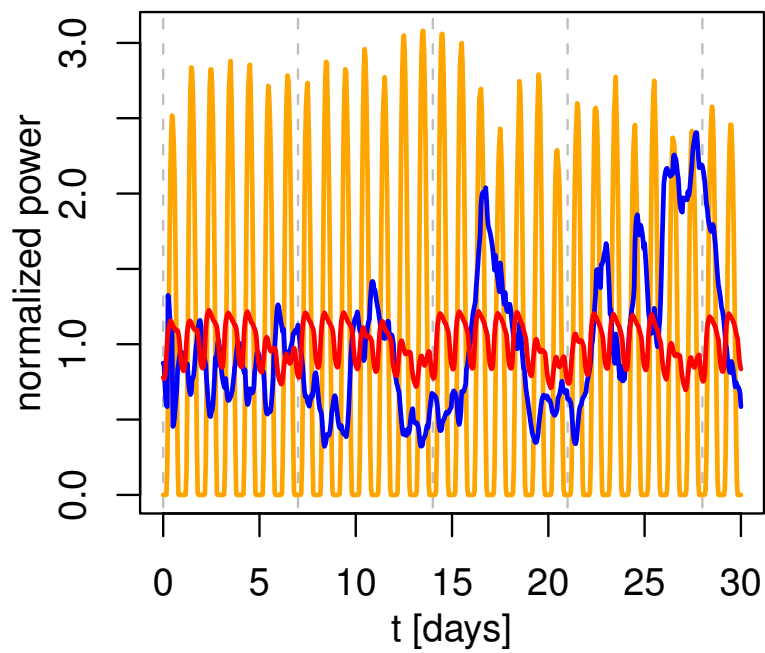
γ	a	$E_H^{\eta=1}$	$E_H^{\eta=0.6}$	E_B	$Q_B^{q=0.9}$	$Q_B^{q=0.99}$	$Q_B^{q=0.999}$
1	0.6	0.101	—	0.198	0.554	0.807	0.973
	0.7	0.116	—	0.166	0.501	0.759	0.931
	0.8	0.147	—	0.153	0.465	0.718	0.899
	0.9	0.182	—	0.163	0.479	0.708	0.877
1.25	0.6	0.014	0.069	0.129	0.452	0.724	0.897
	0.7	0.013	0.043	0.100	0.386	0.668	0.849
	0.8	0.017	0.050	0.084	0.337	0.624	0.817
	0.9	0.034	0.078	0.089	0.343	0.610	0.788
1.5	0.6	0.005	0.019	0.087	0.356	0.649	0.834
	0.7	0.005	0.015	0.063	0.280	0.588	0.784
	0.8	0.007	0.018	0.049	0.218	0.541	0.745
	0.9	0.015	0.037	0.050	0.218	0.526	0.716

Table 2: Same as Table 1, but based on daily instead of hourly mismatches.

γ	a	$E_H^{\eta=1}$	$E_H^{\eta=0.6}$	E_B	$Q_B^{q=0.9}$	$Q_B^{q=0.99}$	$Q_B^{q=0.999}$
1	0.6	0.100	—	0.094	0.292	0.549	0.648
	0.7	0.115	—	0.110	0.331	0.557	0.666
	0.8	0.147	—	0.129	0.379	0.583	0.695
	0.9	0.182	—	0.151	0.436	0.633	0.745
1.25	0.6	0.014	0.034	0.028	0.103	0.388	0.503
	0.7	0.013	0.025	0.037	0.156	0.407	0.526
	0.8	0.016	0.035	0.055	0.221	0.447	0.570
	0.9	0.034	0.071	0.077	0.297	0.528	0.635
1.5	0.6	0.004	0.010	0.009	0.000	0.246	0.364
	0.7	0.005	0.009	0.012	0.000	0.275	0.395
	0.8	0.006	0.011	0.021	0.074	0.316	0.444
	0.9	0.015	0.035	0.038	0.164	0.438	0.540



(a)



(b)

Figure 1: Normalized (blue) wind power generation, (yellow) solar power generation and (red) load, with spatial aggregation over Europe. (a) One-day resolution over one year, and (b) one-hour resolution over one month. See Ref. [1] for modeling details. The vertical dashed lines indicate months and weeks, respectively.

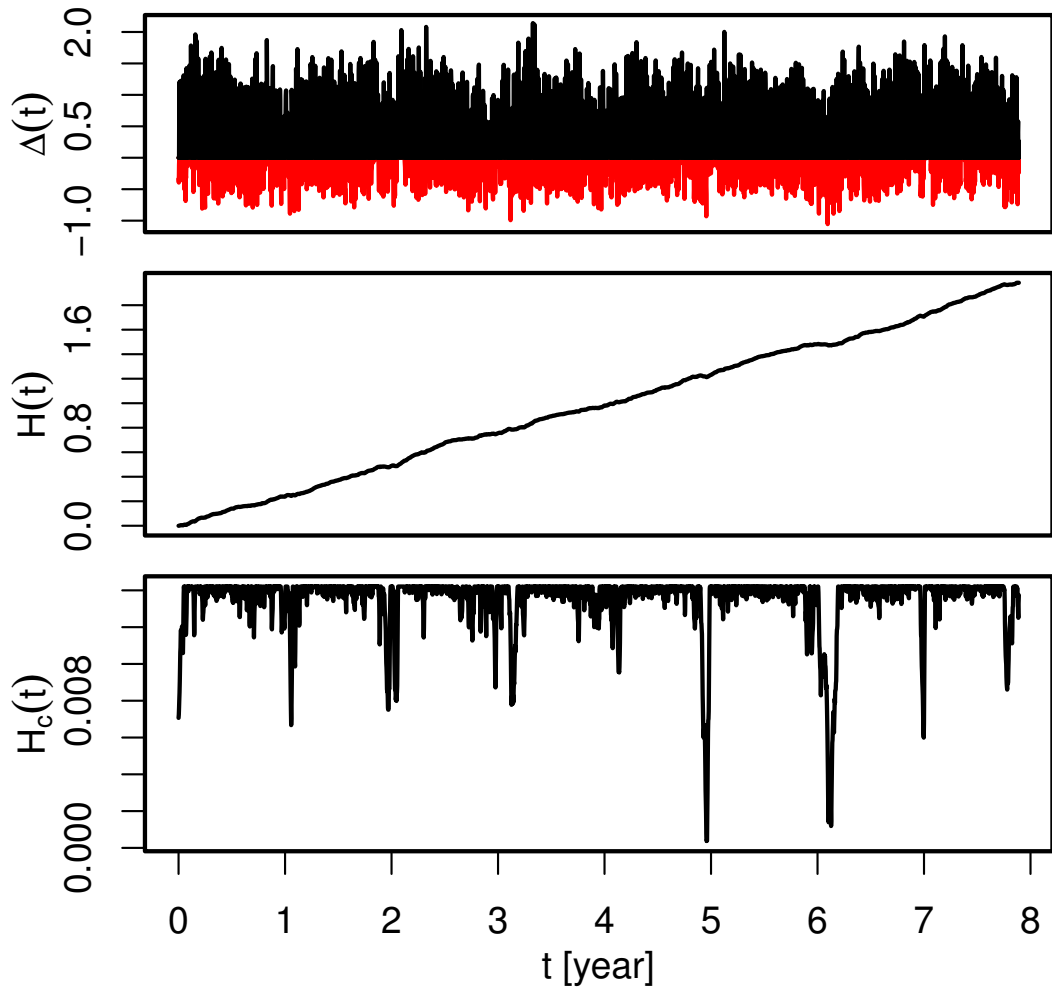


Figure 2: Time series of (top) positive (black) and negative (red) power mismatch (2.1), (middle) non-constrained storage level (2.2), and (bottom) storage level (2.4) constrained with (2.3). The unit of the power mismatch is given in average hourly load. The unit of the storage levels is given in annual consumption. Parameters have been set $\gamma = 1.25$, $a = 0.60$, $\eta_{\text{in}} = \eta_{\text{out}} = 1$.

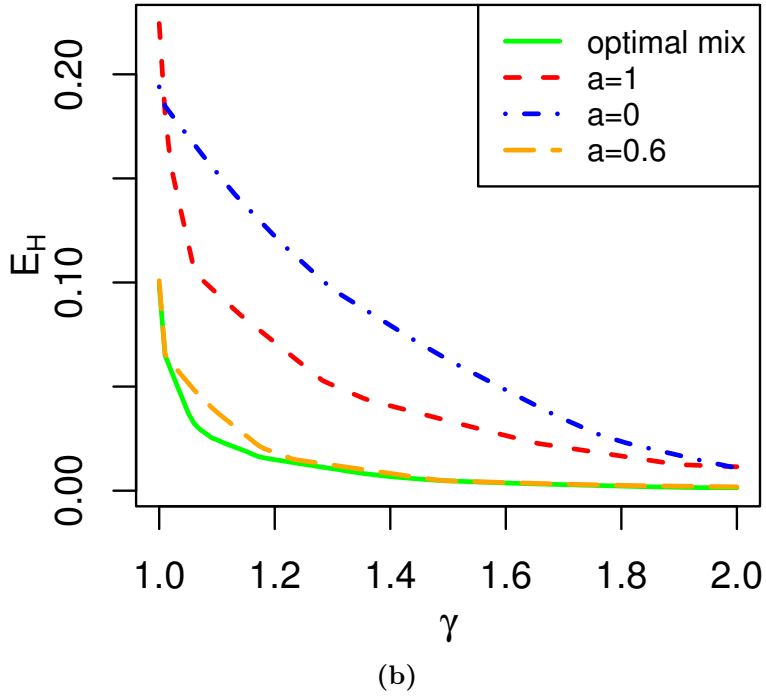
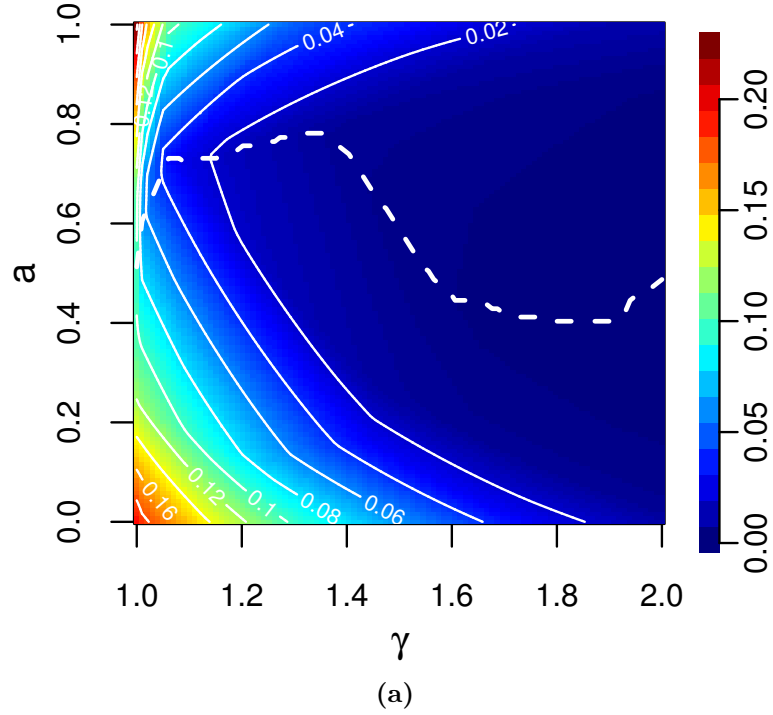


Figure 3: (a) Storage energy capacity (2.3) as a function of the excess generation γ and the share a of wind power generation. The storage efficiencies have been set equal to $\eta_{in} = \eta_{out} = 1$. The contour lines represent constant storage energy capacity and their attached numbers are measured in average annual consumption. The dashed line indicates the optimal mix. (b) Cuts through (a) at $a = 1.0$ (red), 0.6 (orange), 0.0 (blue), and along the dashed optimal-mix line (green).

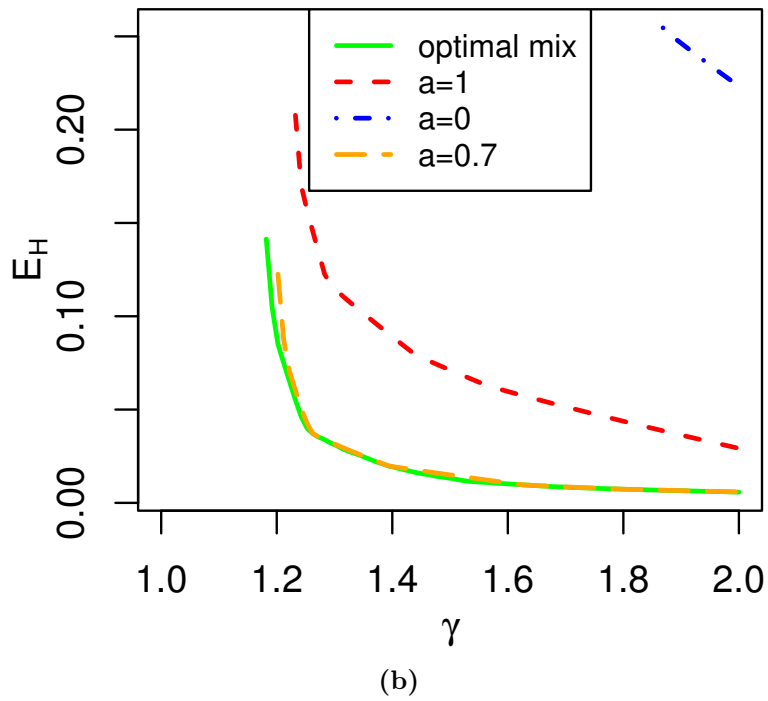
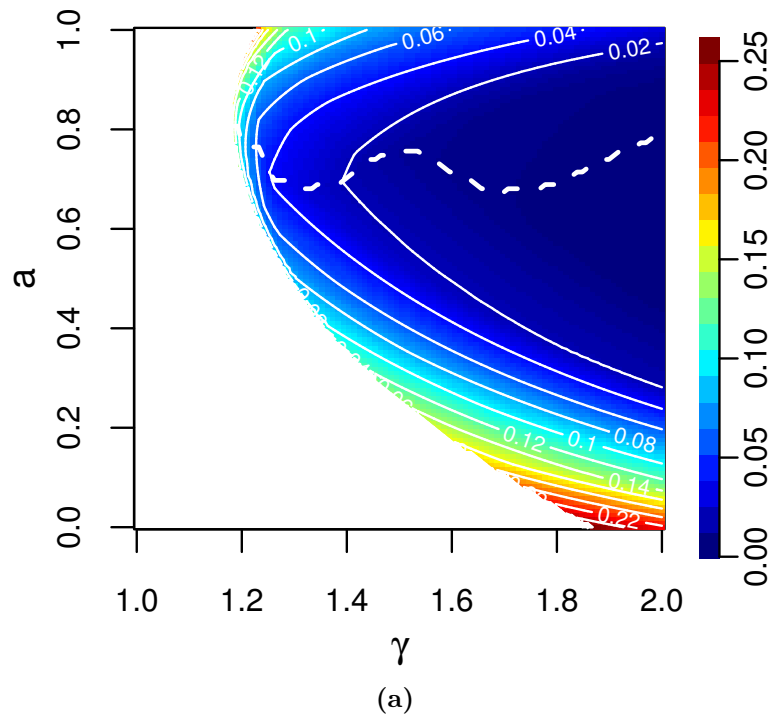


Figure 4: Same as Fig. 3, but for storage efficiencies $\eta_{in} = \eta_{out} = 0.6$.

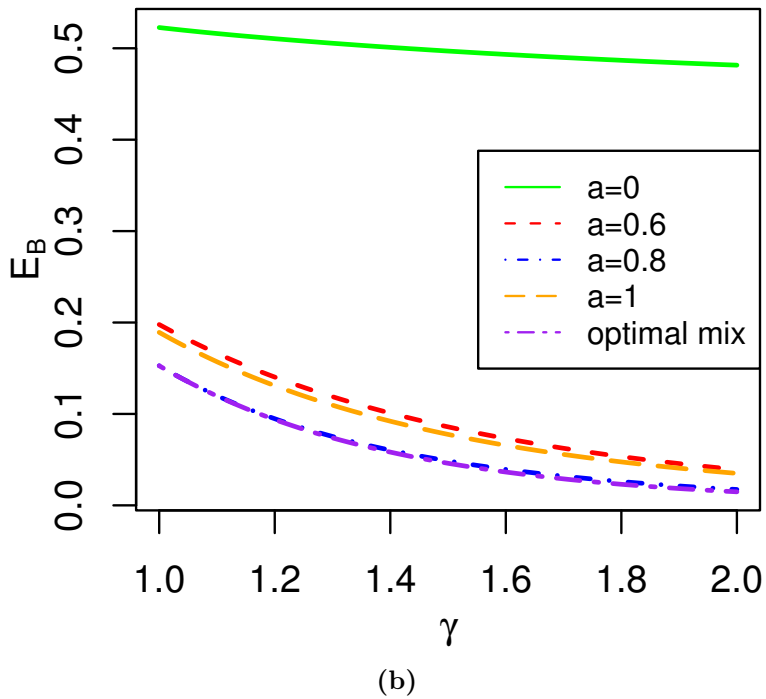
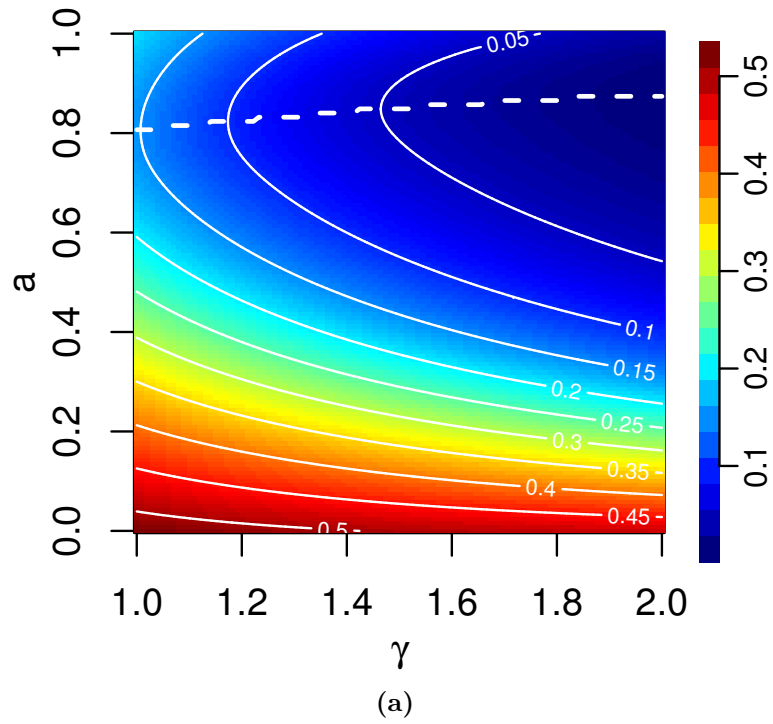


Figure 5: (a) Annual balancing energy (3.2) as a function of the excess generation γ and the share a of wind-power generation. The contour lines represent constant balancing energy and their attached numbers are measured in annual consumption. (b) Cuts through (a) at $a = 1.0$ (yellow), 0.8 (blue), 0.6 (red), 0.0 (green), and along the dashed optimal-mix line (purple).

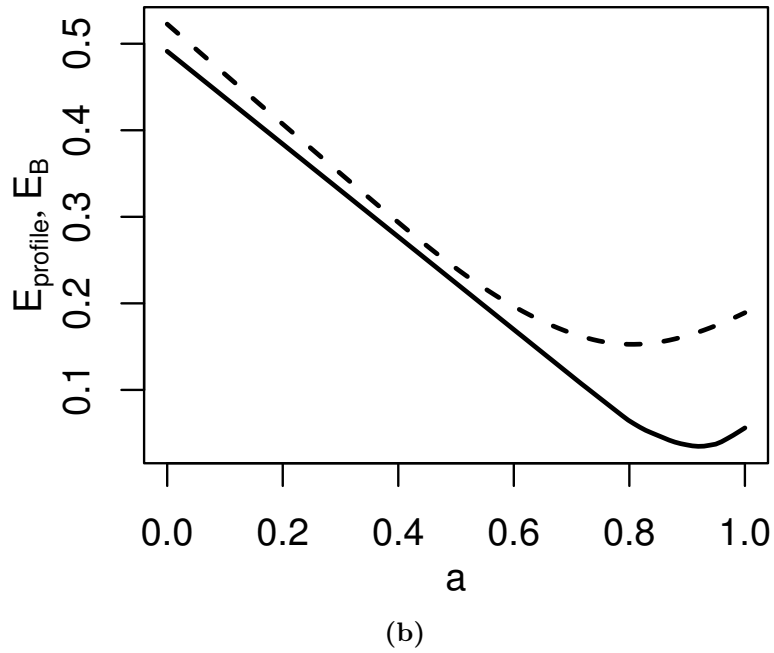
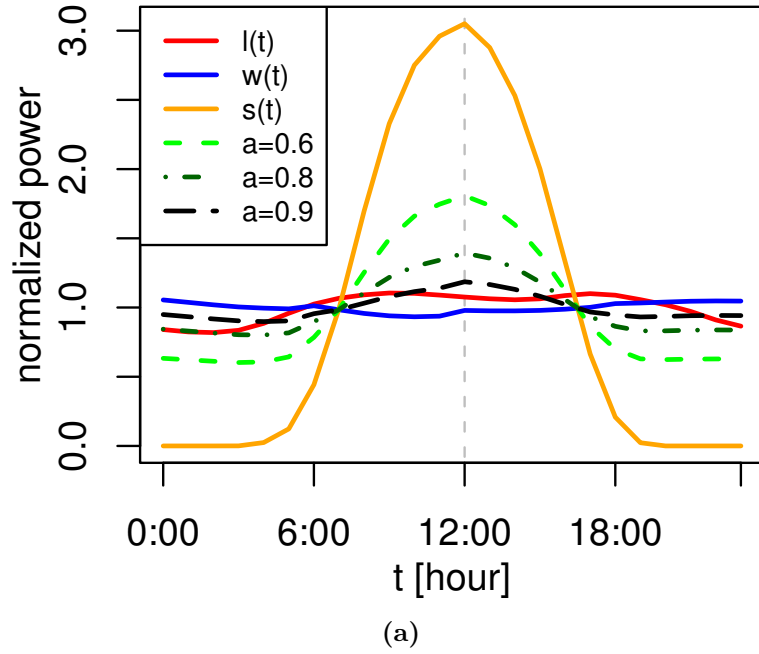
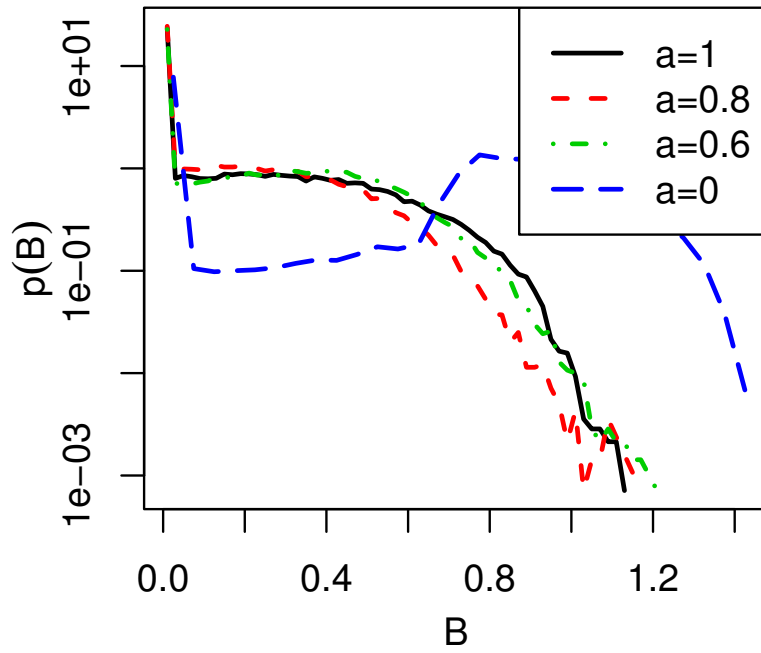
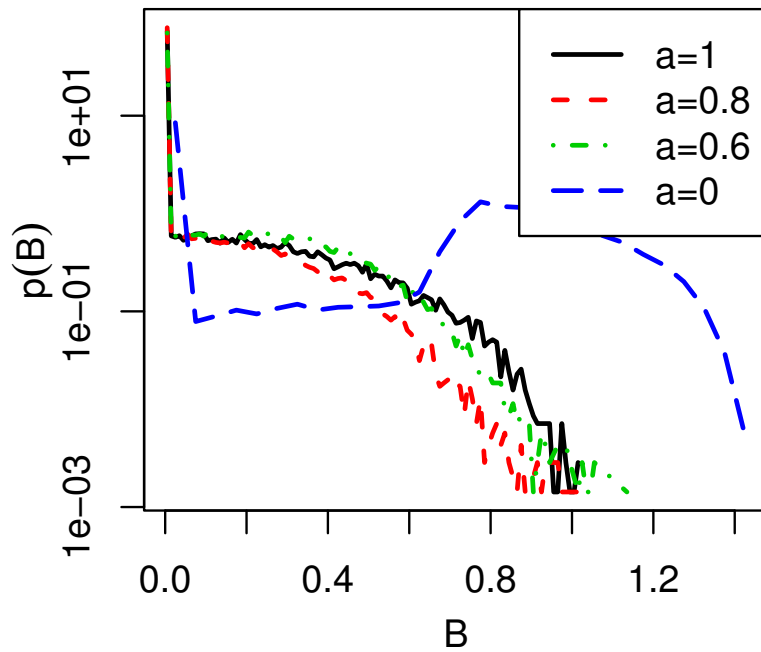


Figure 6: (a) Average daily profiles of (red) load, (blue) wind power generation, (yellow) solar power generation, (dashed green) 60%/40%, (dash-dotted dark-green) 80%/20% and (long-dashed black) 90%/10% mix of wind/solar power generation. The profiles have been averaged over 8 years and are normalized to one. (b) Balancing measure (3.3) as a function of the share a of wind-power generation. The excess generation has been fixed to $\gamma = 1$. For comparison, the balancing energy (3.2) with $\gamma = 1$ is shown as the dashed curve.



(a)



(b)

Figure 7: Probability distributions $p(B)$ of hourly balancing power (3.1) for $a = 1.0, 0.8, 0.6, 0.0$ and $\gamma = 1.0$ (a), 1.5 (b). The probability distributions have been sampled over eight years. The unit of the balancing power is the average hourly load.

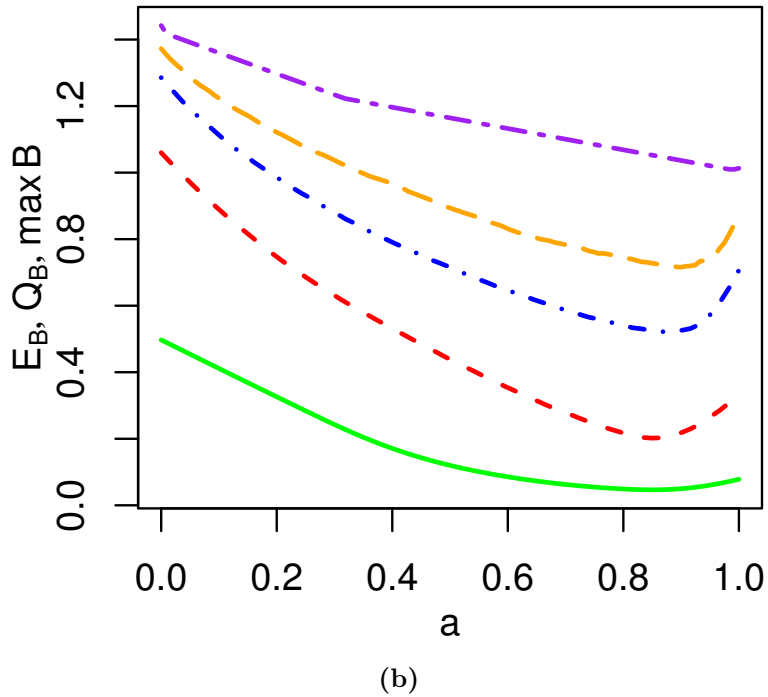
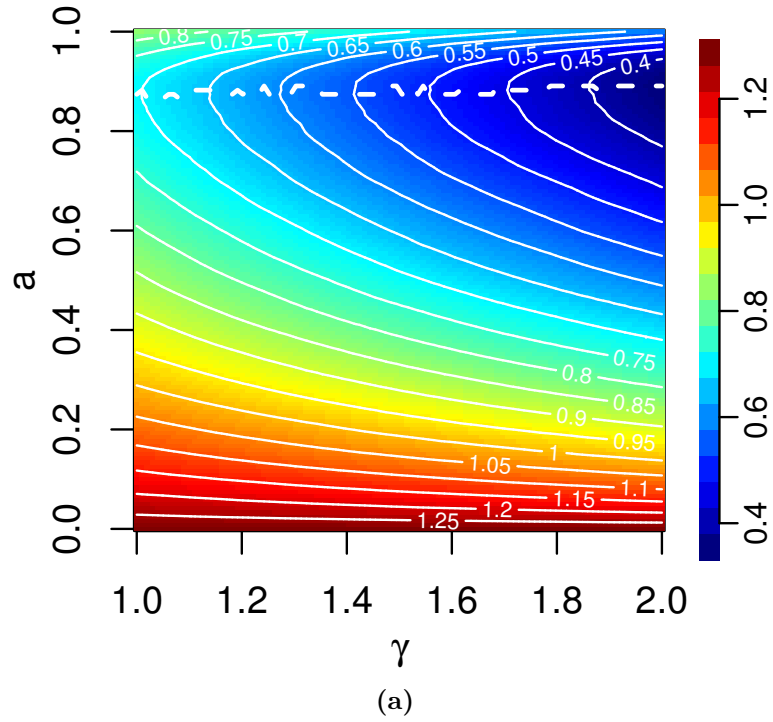


Figure 8: (a) 99% hourly-balancing quantile Q_B as a function of a and γ . (b) From top to bottom, maximum balancing power $\max_t B(t)$, 99.9%, 99% and 90% quantiles Q_B , as well as the average balancing energy E_B as a function of a for fixed $\gamma = 1.5$. The unit of the balancing quantiles is the average hourly load. For the average balancing energy the unit is the average annual consumption.

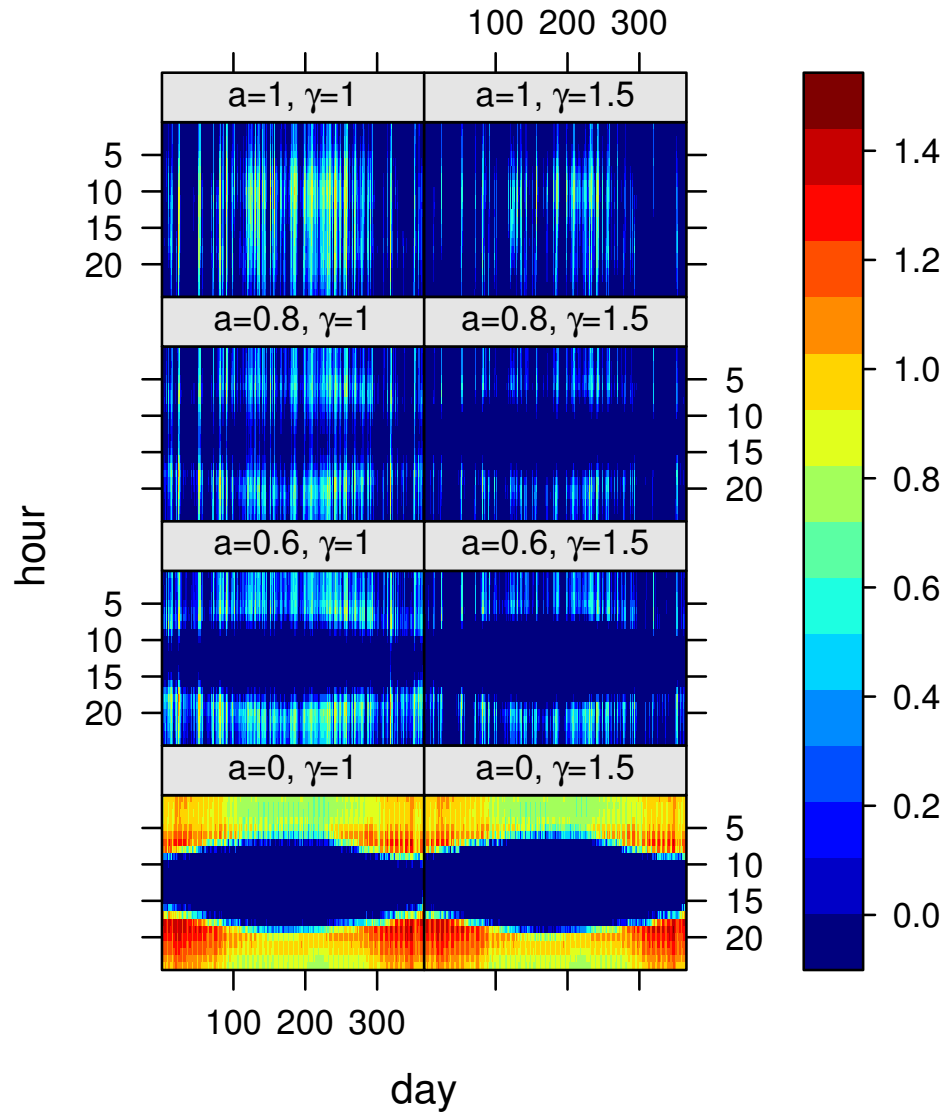


Figure 9: Fluctuation pattern of balancing power over all hours (y -axis) and days (x -axis) within one arbitrary year. Eight different combinations for a and γ are shown. The unit of the balancing power is given in average hourly load.

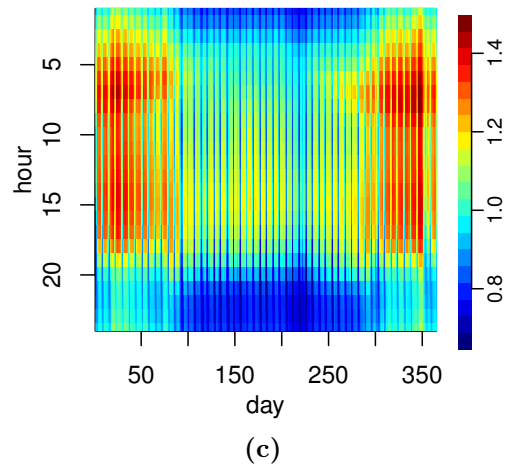
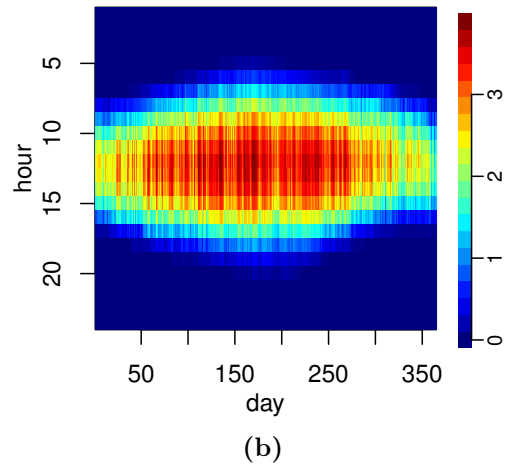
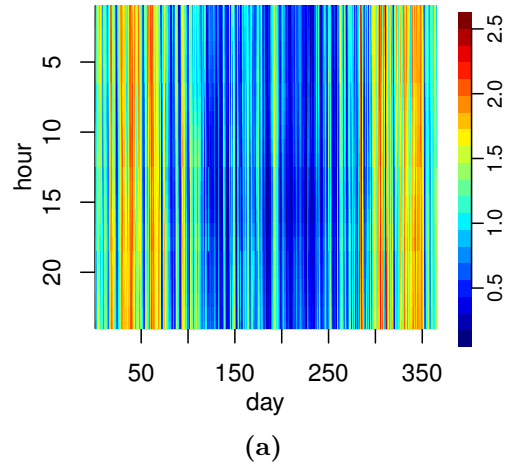


Figure 10: Fluctuation pattern of (a) wind power generation, (b) solar power generation and (c) load over all hours and days within one arbitrary year. The units are the respective average hourly values.

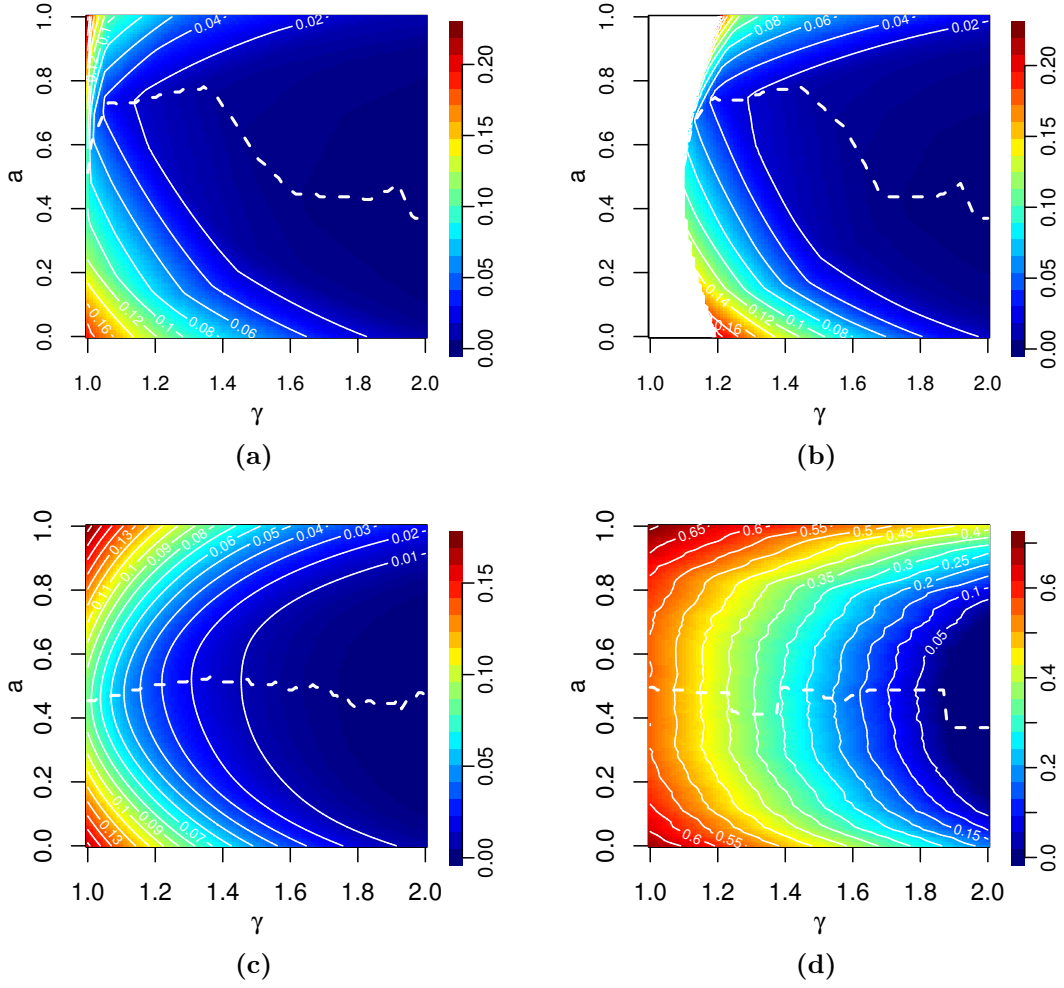


Figure 11: Storage energy capacity E_H with (a) $\eta_{in} = \eta_{out} = 1$ and (b) $\eta_{in} = \eta_{out} = 0.6$, (c) annual balancing energy E_B and (d) 99% balancing quantile Q_B based on the daily mismatch (5.2) and balancing power (5.3). The unit of the contour lines for the storage energy capacity and balancing energy is the average annual consumption. The unit of the contour lines for the balancing quantile is the average hourly load.

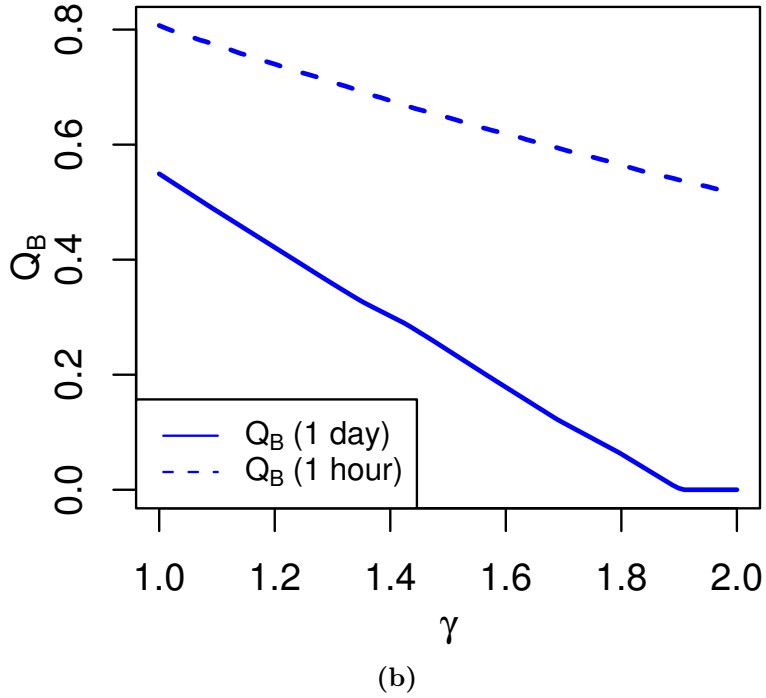
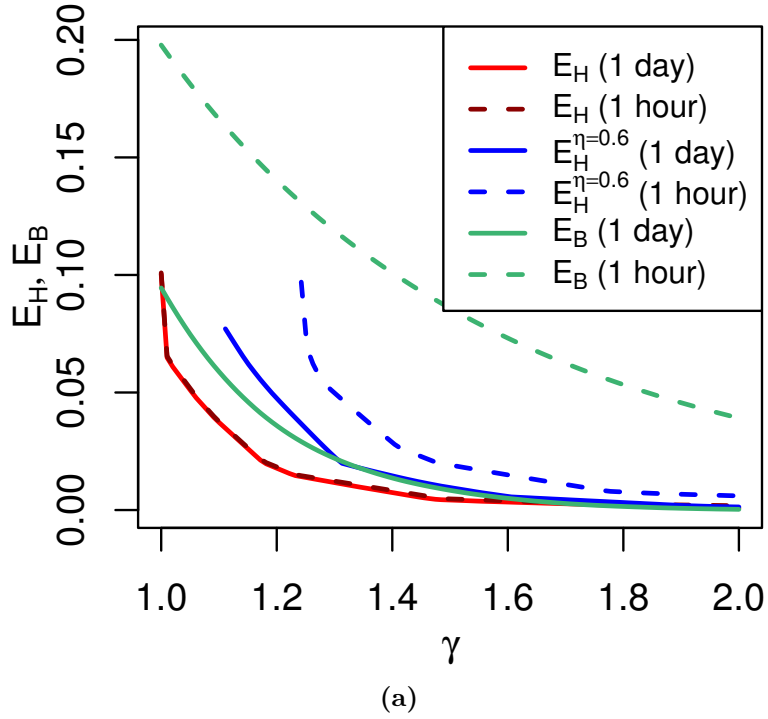


Figure 12: Comparison of the differing impacts between (dashed) hourly and (solid) daily mismatches (2.1) and (5.2) on (a) storage energy capacity E_H with (red) $\eta_{in} = \eta_{out} = 1$ and (blue) $\eta_{in} = \eta_{out} = 0.6$, (green) annual balancing energy E_B , and (b) 99% balancing quantile Q_B . The unit of the storage energy capacity and balancing energy is given in average annual load. The unit of the balancing quantiles is given in average hourly load. The parameter a has been fixed to $a = 0.6$.